Regulating lithium nucleation and growth by zinc modified current collectors

Na Zhang¹, Seung-Ho Yu^{1,2} (🖂), and Héctor D. Abruña¹ (🖂)

- ¹ Baker Laboratory, Department of Chemistry and Chemical Biology, Cornell University, Ithaca, New York, 14853, USA
- ² Department of Chemical and Biological Engineering, Korea University, 145 Anam-ro, Seongbuk-gu, Seoul 02841, Republic of Korea

© Tsinghua University Press and Springer-Verlag GmbH Germany, part of Springer Nature 2019 **Received:** 26 September 2019 / **Revised:** 3 November 2019 / **Accepted:** 10 November 2019

ABSTRACT

Lithium metal is commonly regarded as the "Holy Grail" anode material for high energy density rechargeable batteries. However, the uncontrollable growth of Li dendrites has posed safety concerns and thus greatly hindered its large-scale application. Here we have modified the surface of a commercial anode current collector, Cu foil, with a thin layer of Zn by a facile electroplating method, in order to regulate the Li nucleation and the following growth processes. Because of the formation of a solid solution buffer layer and Li-Zn alloy phases, the Li nucleation overpotential was dramatically reduced, realizing a uniform Li nucleation and a smooth Li plating morphology. As a result, significantly improved long-term cycling performance with a high Coulombic efficiency was achieved by the lithiophilic Zn coated Cu foil as a current collector. Full cells of Li–LiFePO₄ and Li–S using the Li deposited on the Zn modified Cu as the anode, showed increased capacity with low voltage hysteresis and greatly enhanced cycling stability, ascribed to the uniform Li deposition and formation of a stable SEI layer. This work demonstrates the feasibility of employing lithiophilic modified Cu foils as Li metal current collectors for practical applications.

KEYWORDS

lithium metal anode, lithium dendrite, current collector, zinc layer

1 Introduction

With the ever-increasing demand for high energy-density, safe and economical energy sources for portable electronics, electric vehicles and grid storage, tremendous efforts have been devoted to developing rechargeable batteries [1, 2]. Conventional lithium ion batteries, using graphite as anodes, have been widely used for decades, but are approaching their theoretical energy density limit and are unable to meet the rising energy demands [3–6]. Advanced rechargeable batteries, including Li-sulfur, Li-air and Li-selenium batteries, are being actively pursued owing to their high energy density and cost-effectiveness, compared to lithium ion batteries [5-9]. To fulfill their promise as high energy devices, they will require the use of anode materials with high energy density. Metallic lithium is the most attractive anode material and regarded as the "Holy Grail" for these advanced electrical energy storage devices, because Li possesses the highest theoretical specific capacity of 3,860 mAh·g⁻¹ and the lowest negative electrochemical potential (-3.04 V versus the standard hydrogen electrode) [4, 10, 11]. Even though lithium metal batteries were fabricated half a century ago [2], this technology was suspended for decades and even today, it has not yet achieved commercialization. This is due to the intrinsic challenges associated with Li cycling. The highly reactive Li metal is prone to react with organic electrolytes to form an unstable solid electrolyte interphase (SEI) [12] between the electrode and the electrolyte [13]. In addition, the "hostless" nature of lithium metal makes it suffer from significant volumetric changes, leading to cracks of the SEI layer and, again, exposing fresh Li to the electrolyte to form a new SEI layer [13, 14]. The continuous consumption of active Li and electrolyte reduces the Coulombic efficiency and rapidly shortens the cycle life. More importantly, the lithium ions tend to deposit on current collectors unevenly, resulting in the formation of uncontrollable lithium dendrites [14–16]. The growth of Li dendrites during cycling induces serious problems, including capacity loss with "dead lithium" [17–19], potential internal short circuits and thermal runaway with the attendant safety concerns [20].

Researchers have investigated the deposition processes of lithium and explored various strategies to tackle these issues. Solid electrolytes, based on inorganic or polymer materials, have been studied for decades to mechanically block dendrite growth [21-25]. However, the low ionic conductivity of solid electrolytes, compared to that of liquid electrolytes [26] and the large solid-solid interfacial impedance [27], makes it difficult to achieve high power densities at room temperature. Recently, numerous studies have been conducted to suppress lithium dendrites and stabilize the SEI layer by optimizing components of the electrolyte or employing various additives [28-32]. However, the continuous consumption of most additives during cycling makes the suppression approach unsustainable for long term cycling. Another strategy is the fabrication of a porous matrix, such as 3D porous Cu [33], to reduce the local current density and accommodate more Li in the host, in order to control the morphology of Li deposition [34-39]. But the construction of such porous hosts usually involves complex procedures and high temperature treatment, which is time-consuming and economically inefficient for large-scale production. Alternatively,



some work has focused on protecting the lithium metal surface by stable artificial interlayer materials, such as MoS₂ [40], ultrathin boron nitride [41, 42] or polymers [43], to inhibit the reaction between the Li metal surface and the electrolyte. Recently, the Cui group demonstrated that a "lithiophilic" matrix is preferred for Li metal nucleation [16]. They found that no overpotential is needed for Li nucleation on the surface of metals such as Ag, Pt, Ag, Zn and Mg. The elimination of the nucleation barriers is due to the solubility of the substrate in Li and the formation of a solid solution buffer layer for subsequent Li metal deposition. It would be of significance to explore the Li cycling performance on current collectors modified by these lithiophilic materials. In addition, copper foils are commonly used as the current collector for anodes in the battery industry. However, very few efforts have been devoted to the fabrication and investigation of lithiophilic Cu foils in detail [44-46].

Herein, we have developed a facile method to modify Cu foil by coating the surface with a thin layer of electrodeposited Zn. The Zn layer on the Cu foil can serve as a lithiophilic layer to regulate Li nucleation, and therefore, inhibit Li dendrite formation. With the introduction of the lithiophilic Zn coating layer, the Li nucleation overpotential is greatly reduced, compared to pristine Cu foils, owing to the formation of Li-Zn alloys as well as a solid solution buffer layer. The uniform Li nucleation gives rise to a flat and smooth Li deposition without Li dendrite formation. Further electrochemical studies revealed that the thickness of the Zn layer is an important factor to determine the cycling performance. Greatly enhanced Coulombic efficiencies, during stripping/plating of lithium metal, have been achieved with the appropriate Zn thickness. When paired with a commercial LiFePO₄ or a sulfur cathode, Li deposited on the Zn modified Cu current collector as the anode, demonstrated better cycling stability with higher capacity retention when compared to a pristine Cu foil.

Experimental

2.1 Coating copper foils with zinc

A copper foil and a zinc foil were placed in a beaker cell. 0.5 M of Zn(NO₃)₂ solution was used as the electrolyte. By applying a constant current density (0.5 mA·cm⁻²) for a prescribed time (30 s, 1 min, 1 min 30 s, 2 min, 3 min), a layer of zinc was deposited on the surface of the Cu foil. The obtained Zn coated Cu foil was rinsed with deionized water. The thickness of the Zn layer could be controlled by the deposition time.

2.2 Electrochemical measurements

Coin cells were assembled with pristine Cu foils or Zn coated Cu foils as a working electrode and a Li foil as a counter/ reference electrode. 1 M LiPF₆ in ethylene carbonate (EC) and diethyl carbonate (DEC) (1:1, by volume) was used as the electrolyte to study Li nucleation and deposition processes in the cells. Galvanostatic charge/discharge tests were performed on an Arbin battery cycler (Arbin, BT 2000, USA). To test the performance efficiency, the working electrode was first deposited with Li at a current density of 1 mA·cm⁻² for 2 h and then stripped to a cutoff voltage of 0.8 V (vs. Li⁺/Li) at the same current density. The Coulombic efficiency (CE) was calculated from the ratio of Li stripping to deposition, as shown by the equation: $CE = Q_{\text{stripping}}/Q_{\text{deposition}} \times 100\%$. Full cells were assembled using a pristine Cu foil or a Zn coated Cu foil with predeposited 6 mAh·cm⁻² of Li as the anode and a commercial LiFePO₄ or a sulfur electrode as the cathode. To prepare the

LiFePO₄ electrode, commercial LiFePO₄ power, Super P and polyvinylidene fluoride (PVDF) were mixed at a weight ratio of 8:1:1 to form a homogeneous slurry and then coated onto a carbon coated Al foil. 1 M LiPF₆ in EC/DEC (1:1) was used as the electrolyte. Sulfur electrodes were prepared by mixing commercial sulfur powder, Super P, and PVDF in a mass ratio of 70:25:5. The electrolyte for Li–S was 1 M bis(trifluoromethane) sulfonamide lithium salt (LiTFSI) dissolved in a mixed solvent of 1,3-dioxolane (DOL) and 1,2-dimethoxyethane (DME) (1:1, v/v) with 0.2 M LiNO₃ as an additive. The Li-LiFePO₄ full cells were tested at a rate of 1 C (1 C = 170 mA·g⁻¹) and the Li–S cells were initially activated at a rate of 0.2 C (1 C = 1,675 mA·g⁻¹) for 3 cycles, followed by cycling at 0.5 C.

Structure and morphology characterizations

Field emission scanning electron microscope images were obtained with a Keck SEM (Zeiss 1550 FESEM). To observe the morphology of Li deposited on the current collectors, the cells were disassembled in an Ar-filled glovebox with low H2O and O₂ level (< 0.3 ppm) to extract the electrode, which was subsequently rinsed with dimethyl carbonate (DMC) to remove residual electrolyte and salts.

Results and discussion

Copper foils were coated with Zn via a facile electroplating process. A Cu foil and a Zn foil were placed in a Zn(NO₃)₂ solution and underwent galvanostatic electroplating to deposit a thin layer of Zn on the surface of the copper foil, as illustrated by the scheme in Fig. S1 in the Electronic Supplementary Material (ESM). The scanning electron microscope (SEM) images of the pristine Cu foil and the Zn coated Cu foil are shown in Figs. 1(a) and 1(c), respectively. Compared to the pristine Cu foil, the surface of the Zn coated Cu foil is flatter and smoother, which is beneficial for the subsequent uniform Li nucleation and growth. The thickness of the Zn film was calculated based on Faraday's laws of electrolysis. The Zn layer is too thin (10-50 nm) to be detectable by X-ray diffraction (XRD) (Fig. S2 in the ESM), so that it shows the same XRD patterns before and after the coating. The investigation of dendrite growth was carried out under conditions of Li plating/stripping at a current density of 1 mA·cm⁻² with an areal capacity of 2 mAh·cm⁻², as shown in Figs. 1(b) and 1(d). Direct deposition of Li on the bare Cu foil results in a loose and rough surface with ragged growth of Li filaments, which likely arises from an uneven distribution of the current density along the foil. In sharp contrast, a smooth and dense Li surface is observed on the Zn coated Cu foils, clearly reflecting that Zn can effectively yield a uniform Li growth on the current collectors.

To demonstrate the reversibility and effectiveness of the Zn coated Cu foil for Li deposition, half cells consisting of the modified current collector, as a working electrode, and a lithium foil as a reference/counter electrode were used to study the cycling stability and Coulombic efficiency of Li plating/stripping. 1 M LiPF₆ in 1:1 EC and DEC was used as the electrolyte. The cells were first cycled at a current density of 50 μA·cm⁻² within the voltage range from 0 to 1 V for 3 cycles to stabilize the SEI layer and remove contaminants [37]. The Coulombic efficiency, an important parameter to evaluate the electrochemical performance of Li metal anodes, was calculated by the capacity ratio of Li stripped from the current collector to that during the deposition cycle [47, 48]. As shown in Fig. 1(e), the cell using the bare Cu foil shows a gradual decay in Coulombic efficiency, and an efficiency of only ~ 25% was obtained after

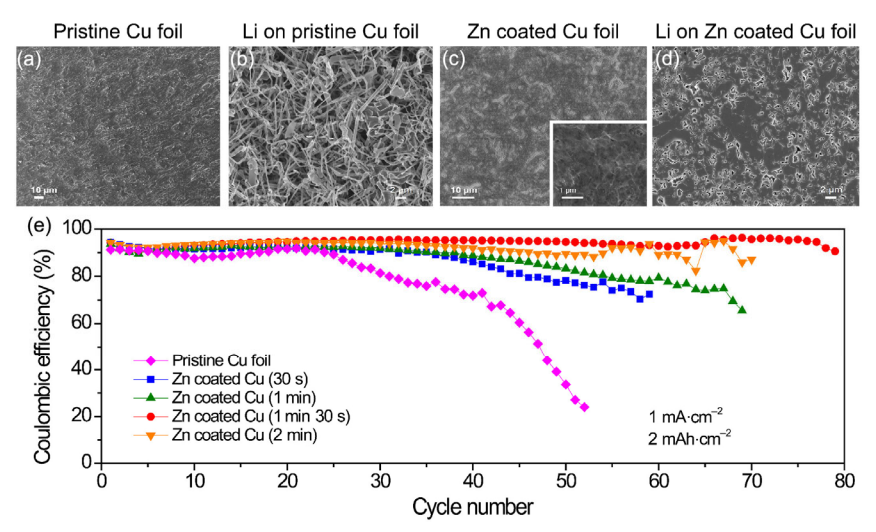


Figure 1 SEM images of (a) a bare Cu foil and (c) a Cu foil coated with Zn by the electroplating method at low magnification and at high magnification (inset). SEM images of Li deposition of 1 mAh·cm⁻² on (b) a bare Cu foil and (d) a Zn modified Cu foil. (e) Comparison of the Coulombic efficiency at a current density of 1 mA·cm⁻² in 1 M LiPF₆ in EC/DEC on a bare Cu foil and on Zn coated Cu foils with different Zn layer thicknesses.

50 cycles at 1 mA·cm⁻² with an areal capacity of 2 mAh·cm⁻², indicating that during the cycling, less and less Li could be stripped off from the bare Cu film. This is likely due, at least in part, to the formation of a large amount of Li dendrites, resulting in "dead Li" which detaches from the current collector [49]. In addition, the increased surface area arising from the formation of mossy Li dendrites, causes the repeated consumption of the electrolyte, leading to its rapid exhaustion. In contrast, for the Zn modified Cu current collector with different Zn deposition times (in other words, different Zn thicknesses), all cells exhibited improved Coulombic efficiency compared to the bare Cu foil. We found that when the Zn deposition time reached 1.5 min and beyond, corresponding to a Zn thickness of ~ 22 nm (by calculation), the Li deposition showed the best stability. The Coulombic efficiency remained at as high as 91% for 80 cycles at 1 mA·cm⁻² with an areal capacity of 2 mAh·cm⁻². This points out that the Zn layer is able to stabilize the long-term platting/stripping performance of deposited Li when the thickness of the Zn is sufficient to suppress Li dendrite growth. It should be noted that no additives were added to the electrolytes in this study and that the alkyl carbonate electrolytes usually show worse cycling performance than ether-based electrolytes for Li deposition [50]. It can be posited that the Coulombic efficiency of our Zn coated Cu foils could be further enhanced in ether-based electrolytes, such as 1 M lithium bis(trifluoromethanesulfonyl) imide (LiTFSI) in 1,3-dioxolane and 1,2-dimethoxyethane (DOL/ DME, 1:1 by volume), or with electrolyte additives such as FEC [51, 52]. The Li plating-stripping performance of symmetric cells on a Zn coated Cu foil and a pristine Cu foil are presented in Fig. S3 in the ESM, which clearly shows a much longer cycling life when using a Zn coated Cu foil as a current collector.

It is important to assess whether the dendrite-free morphology can be maintained after numerous cycles, therefore the Li deposited on the Zn modified Cu current collectors was extracted after 80 cycles (320 h) of stripping/platting. It can be clearly seen from the top-view SEM images of the film in Fig. 2(a) that the Li surface remains smooth and flat. The cross-sectional SEM image (Fig. 2(b)) further illustrates the dense and homogeneous deposit, demonstrating the excellent reversibility of Li deposition/stripping process and the effective suppression of Li dendrites for long-term cycling with a high Coulombic efficiency.

In order to better understand the effects of the Zn layer on suppressing the growth of Li dendrites, the components of the SEI layer were studied. Elemental mapping was conducted on a long-term cycled Li deposited on the Zn modified Cu foil. During disassembling of coin cells, some regions of the film were cracked, exposing the Li underneath the SEI layer. To observe the SEI layer and compare it with the fresh Li underneath, a region containing both areas was selected for elemental mapping (Fig. 2(c)). The mapping results in Fig. 2(d) show distinct differences between the SEI layer and fresh Li. Signals from C, O, F and P were clearly found in the SEI layer instead of in the Li underneath, which are ascribed to electrolyte decomposition during cycling. More significantly, Zn was also detected in the SEI layer. This suggests that Zn likely participates in the formation of the SEI which is quite likely due to the formation of a solid buffer layer and Li-Zn alloy phases during the lithium nucleation and growth processes. Figures 3(a) and 3(b) present the cyclic voltammetric (CV) profiles of half cells containing bare Cu or Zn modified Cu current collectors and Li foil cycled between 0 to 1.5 V at a scan rate of 0.1 mV·s⁻¹ along with the galvanostatic voltage profiles at a current density of 50 μA·cm⁻², from which distinct behaviors are evident. During the cathodic scan of the Zn coated Cu foil (Fig. 3(a)), peaks at 0.9, 0.5 and 0.02 V can be observed in the CV profiles, while a high voltage peak at 0.9 V is likely related to the conversion of ZnO (most likely formed as a thin layer when Zn was deposited in an aqueous environment) to Zn, while the lower voltage peaks likely arise from the alloying reaction of Zn with Li to form different Li_xZn_y phases (e.g., LiZn₄, Li₂Zn₅, LiZn₂, Li₂Zn₃, and LiZn) as well as decomposition of the electrolyte [53, 54]. The formation of ZnO on the surface of the coated was confirmed by the XPS spectrum shown in Fig. S4 in the ESM, which exhibited two peaks located at about 1,024 and 1,047 eV, corresponding to Zn $2p_{3/2}$ and Zn $2p_{1/2}$ of Zn²⁺ in ZnO. Interestingly, there are no evident peaks at low voltages found during the following oxidation, suggesting that the formed alloys cannot be reversibly dealloyed and are stable during the subsequent Li platting/stripping. The broad peak above 1.2 V is related to the conversion of Zn back to ZnO [54]. Similar features can be found in galvanostatic voltage profiles (Fig. 3(b)). During the lithiation process, clear voltage plateaus can be found at about 0.9 and 0.6 V, which likely arise from the conversion of ZnO and the formation of Li-Zn alloys along with the formation of the SEI, as discussed above. The increase of the plateau at the low voltage, as the amount of Zn increased (Zn deposition time) can be attributed to more Zn reacting with Li to form alloys, corresponding well to our interpretation

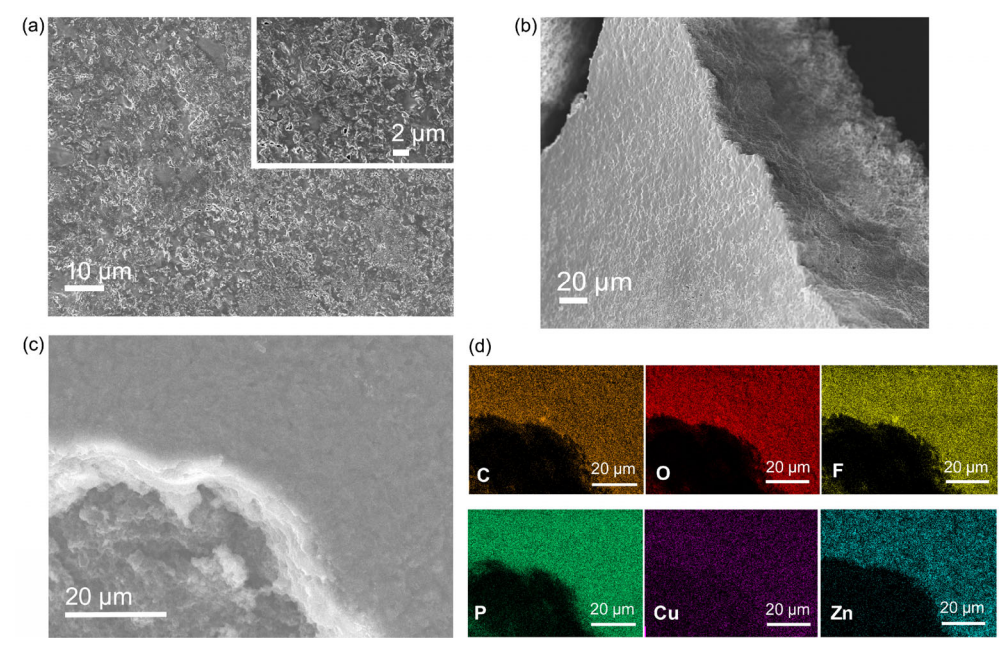


Figure 2 (a) Top-view SEM images of the Li deposited on a Zn coated Cu foil with an areal capacity of 2 mAh·cm⁻² after 80 cycles at low magnification and at high magnification (inset). (b) Cross-sectional SEM image of the deposited Li, where a smooth surface can be observed. (c) Region of the electrode selected for elemental mapping and (d) the corresponding mapping signals from carbon, oxygen, fluorine, phosphorous, copper and zinc. The crack on the electrode exposed the lithium metal underneath the SEI layer, which made it easier to observe the differences between the SEI layer and the Li underneath.

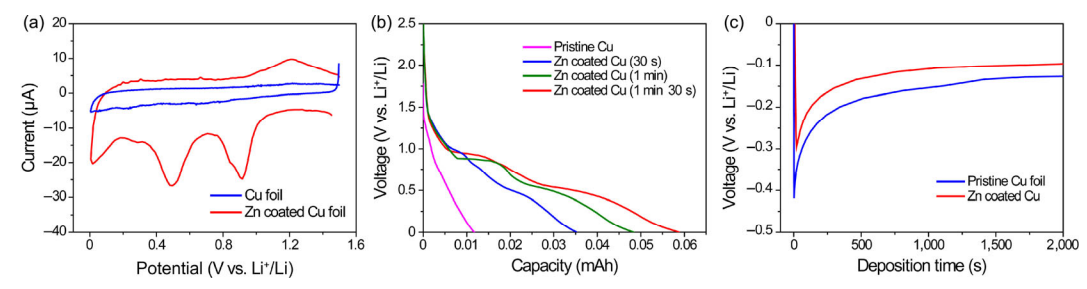


Figure 3 (a) Cyclic voltammograms of the Cu foil and the Zn coated Cu foil in coin cells using 1 M LiPF6 in EC/DEC as the electrolyte and Li as the counter and reference electrodes at a scan rate of 0.1 mV·s⁻¹ with the voltage cutoff between 0 to 1.5 V. (b) Galvanostatic voltage profiles of the cells using pristine/modified Cu foil as the working electrode and Li as the reference/counter electrodes at a current density of 50 μA·cm⁻². (c) Voltage profile of Li nucleation at 1 mA·cm⁻² on a pristine Cu foil and a Zn modified Cu foil.

of the CV profiles. In addition, research has shown that Li prefers to deposit and grow on Li-Zn alloys [16, 55], so the irreversibly produced Li-Zn alloy phases are beneficial for inducing controllable Li nucleation and growth, and thus restrain/ preclude Li dendrite formation.

To further demonstrate the effectiveness of the lithiophillic Zn coated Cu foil in regulating Li nucleation and deposition processes, the overpotentials of Li plating on the bare Cu and the Zn modified Cu foils were investigated at the relatively high current density of 1 mA·cm⁻². The nucleation overpotential can be obtained by comparing the difference between the sharp voltage peaks and the voltage plateaus [56]. At the beginning of Li plating on the bare Cu foil, a sharp voltage drop to -420 mV is observed in Fig. 3(c), which is related to the nucleation processes. The voltage then rises to a relatively stable value of −120 mV, which is the mass transfer controlled overpotential. Thus, for the pristine Cu current collector, the nucleation overpotential is ca. 300 mV. In contrast, the Zn modified Cu foil shows a relatively shallow voltage peak with a nucleation overpotential of 200 mV, which is much smaller than the value for the bare Cu foil. It can be inferred that the Zn layer helps decrease the Li nucleation barrier. As can be seen in the phase diagram of Zn-Li (Fig. S5 in the ESM) [57], Zn can not only form various alloy phases with Li, but more importantly, it has a solubility zone of Zn inside Li. As demonstrated by the Cui group [16], the solubility zone leads to a solid solution buffer layer before the formation of Li metal. Therefore, both the formation of a buffer layer and Li-Zn alloys render the surface of the modified Cu foil lithiophilic, which helps induce the uniform nucleation and homogenous growth of Li, so that the formation of Li filaments is largely suppressed.

The effects of the Zn layer in preventing the Li from growing into long dendritic shapes can be illustrated by the scheme shown in Fig. 4. For the pristine Cu foil, the initial Li nucleation is not uniform as Li prefers to nucleate at the protuberances, where a high local current density further accelerates the growth of Li dendrites, leading to an unstable cycling performance with a low Coulombic efficiency. In contrast, the Zn coating layer favors a more uniform current density on the surface. During the nucleation process, Li will react with Zn to produce Li-Zn alloys and at the same time form a solid solution buffer layer that lowers the Li nucleation barrier, regulating a homogeneous Li nucleation and further controlling the following Li deposition with a stable Zn-containing SEI layer.

In order to explore the possible practical applications of Li deposited on the Zn coated Cu foil, full cells were fabricated using Li deposited on the Zn coated Cu foil or the bare Cu foil as an anode electrode, combined with a commercial cathode

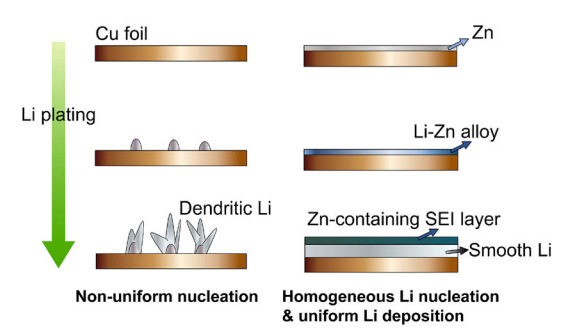


Figure 4 Schematic illustration of the proposed lithium nucleation and deposition processes on a bare Cu foil (left) and a Zn modified Cu foil (right). The rough surface of the bare Cu foil gives rise to non-uniform Li nucleation, which accelerates the growth of dendritic lithium. The Zn layer is able to regulate the homogeneous Li nucleation process by forming a Li-Zn alloy as well as the solid solution buffer layer, which leads to uniform Li growth.

electrode. When paired with a LiFePO4 cathode, the cycling stability of the cells was conducted at a rate of 1 C (1 C = 170 mA·g⁻¹). As evident in Fig. 5(a), the cell using the lithium deposited on the Zn coated Cu foils delivered a higher capacity and better cycling performance up to 100 cycles, while Li on the bare Cu foils showed comparable capacity at first but decayed fast after only 60 cycles. These results illustrate the excellent reversibility of our anode of the Zn modified Cu foils. The voltage profiles for the cells are presented in Fig. 5(b) and Figs. S6(a) and S6(b) in the ESM, where it can be clearly seen that the full cell utilizing Li on Zn coated Cu foil had a stable performance and a reduced voltage hysteresis between charge and discharge cycles (Fig. S6(b) in the ESM). Furthermore, a Li metal battery utilizing deposited Li as the anode and a sulfur electrode as the cathode was tested at 0.5 C (1 C = 1,675 mA·g⁻¹) for 100 cycles. Figures 5(c) and 5(d) show that the cell with Li on Zn modified Cu as the anode, had a higher capacity and significantly improved cycling stability when compared to Li on the bare Cu foil. With a Zn-containing SEI on the Li surface, the SEI is more stable and in addition, due to the suppression of Li dendrites, the surface area is much smaller when compared to Li grown on the bare Cu, so that it lowers the possibility of lithium polysulfies reacting with the Li anode. In contrast, Li grown on pristine Cu foils presents severe dendrite formation, augmenting the surface area and accelerating the reaction of lithium polysulfides with active Li metal. The continuous polysulfides shuttle and corrosion of the Li anode on pristine Cu foils leads to a fast capacity decay and short cycle life. A similar effect of a protective layer on the anode to improve Li-S batteries performance has also been reported by the Choi group [40]. It should be noted that the sulfur cathodes used in our full cell test were obtained by simply mixing 70 wt.% commercial sulfur with Super P and binder, without any other special treatment such as melt-diffusion. The Li-S full cell tests indicate that our Zn coated Cu current collector can not only control the nucleation and growth of Li, but also enhance the cycling performance in Li-S batteries that are considered as one of the most promising candidates for next-generation rechargeable batteries.

4 Conclusions

We have demonstrated a facile method to modify Cu foils as Li metal anode current collectors by electrodepositing a thin layer of Zn on the surface, serving as a lithiophilic layer to regulate the nucleation and growth of Li metal. With the Zn coating layer, the Coulombic efficiencies of plating/stripping

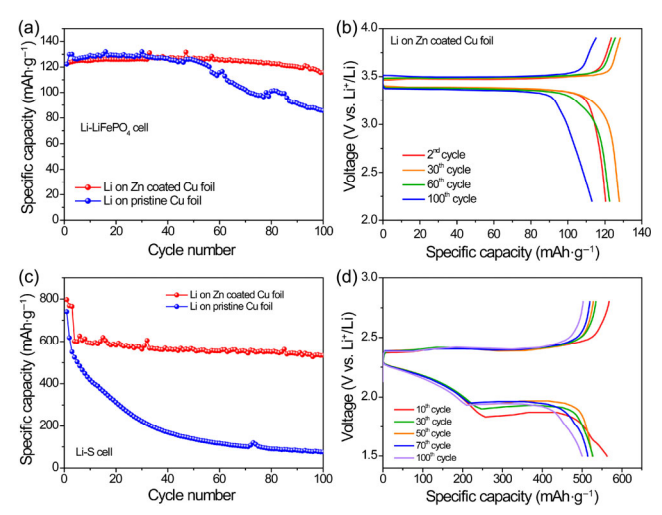


Figure 5 (a) Cycling performance of Li-LiFePO₄ full cells at a rate of 1 C with Li pre-deposited on a pristine Cu foil or a Zn coated Cu foil as the anode. (b) Voltage profiles of the Li-LiFePO₄ full cell using Li deposited on a Zn modified Cu foil as the anode for different cycles at 1 C. (c) Cycling performance of Li–S full cells tested at 0.2 C for the first 3 cycles and at 0.5 C for the subsequent cycles. (d) Voltage profiles of the Li–S cell using Li on the Zn modified Cu foil as the anode for different cycles.

were higher and more stable than on a bare (pristine) Cu foil. The nucleation overpotential was greatly reduced and the long-term cycling stability was significantly enhanced. Full cells using deposited Li and LiFePO $_4$ or sulfur were fabricated, demonstrating the feasibility of using Zn coated Cu foils as Li metal current collectors in practical applications. Considering the facile and low-cost preparation process, the introduction of a coating layer of Zn by electroplating can easily improve the morphology and performance of metallic Li. Thus, the method presented here is suitable for large-scale application and can also be applied to other reported 3D current collectors to further inhibit Li dendrite formation and improve the stripping/ platting performance of the deposited Li metal and this enables lithium metal anodes.

Acknowledgements

This work made use of the Cornell Center for Materials Research (CCMR) Shared Facilities with funding from the NSF MRSEC program [DMR-1719875].

Electronic Supplementary Material: Supplementary material (XRD patterns, XPS spectrum, full cell test) is available in the online version of this article at https://doi.org/10.1007/s12274-019-2567-5.

References

- [1] Armand, M.; Tarascon, J. M. Building better batteries. *Nature* **2008**, 451, 652–657
- [2] Tarascon, J. M.; Armand, M. Issues and challenges facing rechargeable lithium batteries. *Nature* 2001, 414, 359–367.
- [3] Lu, Y.; Yu, L.; Lou, X. W. Nanostructured conversion-type anode materials for advanced lithium-ion batteries. *Chem* 2018, 4, 972–996.
- [4] Xu, W.; Wang, J. L.; Ding, F.; Chen, X. L.; Nasybulin, E.; Zhang, Y. H.; Zhang, J. G. Lithium metal anodes for rechargeable batteries. *Energy Environ. Sci.* 2014, 7, 513–537.
- [5] Bruce, P. G.; Freunberger, S. A.; Hardwick, L. J.; Tarascon, J. M. Li-O₂ and Li-S batteries with high energy storage. *Nat. Mater.* 2012, 11, 19–29.
- [6] Yu, S. H.; Feng, X. R.; Zhang, N.; Seok, J.; Abruña, H. D. Understanding conversion-type electrodes for lithium rechargeable batteries. Acc. Chem. Res. 2018, 51, 273–281.

- [7] Zhang, N.; Levin, B. D. A.; Yang, Y.; Muller, D. A.; Abruña, H. D. Porous Fe₃O₄ nanospheres as effective sulfur hosts for Li–S batteries. *J. Electrochem. Soc.* 2018, 165, A1656–A1661.
- [8] Zhang, N.; Yang, Y.; Feng, X. R.; Yu, S. H.; Seok, J.; Muller, D. A.; Abruña, H. D. Sulfur encapsulation by MOF-derived CoS₂ embedded in carbon hosts for high-performance Li–S batteries. *J. Mater. Chem.* A 2019, 7, 21128–21139.
- [9] Zhang, J. T.; Li, Z.; Chen, Y.; Gao, S. Y.; Lou, X. W. D. Nickel-iron layered double hydroxide hollow polyhedrons as a superior sulfur host for lithium-sulfur batteries. *Angew. Chem., Int. Ed.* 2018, 57, 10944–10948.
- [10] Cheng, X. B.; Zhang, R.; Zhao, C. Z.; Zhang, Q. Toward safe lithium metal anode in rechargeable batteries: A review. *Chem. Rev.* 2017, 117, 10403–10473.
- [11] Lin, D. C.; Liu, Y. Y.; Cui, Y. Reviving the lithium metal anode for high-energy batteries. *Nat. Nanotechnol.* 2017, 12, 194–206.
- [12] Peled, E. The electrochemical behavior of alkali and alkaline earth metals in nonaqueous battery systems—the solid electrolyte interphase model. J. Electrochem. Soc. 1979, 126, 2047–2051.
- [13] Cheng, X. B.; Zhang, R.; Zhao, C. Z.; Wei, F.; Zhang, J. G.; Zhang, Q. A review of solid electrolyte interphases on lithium metal anode. *Adv. Sci.* 2016, 3, 1500213.
- [14] Liu, J.; Bao, Z. A.; Cui, Y.; Dufek, E. J.; Goodenough, J. B.; Khalifah, P.; Li, Q. Y.; Liaw, B. Y.; Liu, P.; Manthiram, A. et al. Pathways for practical high-energy long-cycling lithium metal batteries. *Nat. Energy* 2019, 4, 180–186.
- [15] Cohen, Y. S.; Cohen, Y.; Aurbach, D. Micromorphological studies of lithium electrodes in alkyl carbonate solutions using *in situ* atomic force microscopy. *J. Phys. Chem. B* 2000, 104, 12282–12291.
- [16] Yan, K.; Lu, Z. D.; Lee, H. W.; Xiong, F.; Hsu, P. C.; Li, Y. Z.; Zhao, J.; Chu, S.; Cui, Y. Selective deposition and stable encapsulation of lithium through heterogeneous seeded growth. *Nat. Energy* 2016, 1, 16010.
- [17] Steiger, J.; Kramer, D.; Mönig, R. Mechanisms of dendritic growth investigated by in situ light microscopy during electrodeposition and dissolution of lithium. J. Power Sources 2014, 261, 112–119.
- [18] Chen, K. H.; Wood, K. N.; Kazyak, E.; LePage, W. S.; Davis, A. L.; Sanchez, A. J.; Dasgupta, N. P. Dead lithium: Mass transport effects on voltage, capacity, and failure of lithium metal anodes. *J. Mater. Chem. A* 2017, 5, 11671–11681.
- [19] Lv, S. S.; Verhallen, T.; Vasileiadis, A.; Ooms, F.; Xu, Y. L.; Li, Z. L.; Li, Z. C.; Wagemaker, M. *Operando* monitoring the lithium spatial distribution of lithium metal anodes. *Nat. Commun.* 2018, 9, 2152.
- [20] Aurbach, D.; Gofer, Y.; Langzam, J. The correlation between surface chemistry, surface morphology, and cycling efficiency of lithium electrodes in a few polar aprotic systems. *J. Electrochem. Soc.* 1989, 136, 3198–3205
- [21] Lu, Q. W.; He, Y. B.; Yu, Q. P.; Li, B. H.; Kaneti, Y. V.; Yao, Y. W.; Kang, F. Y.; Yang, Q. H. Dendrite-free, high-rate, long-life lithium metal batteries with a 3D cross-linked network polymer electrolyte. *Adv. Mater.* 2017, 29, 1604460.
- [22] Cheng, X. B.; Yan, C.; Peng, H. J.; Huang, J. Q.; Yang, S. T.; Zhang, Q. Sulfurized solid electrolyte interphases with a rapid Li⁺ diffusion on dendrite-free Li metal anodes. *Energy Storage Mater.* 2018, 10, 199–205.
- [23] Zheng, Q.; Ma, L.; Khurana, R.; Archer, L. A.; Coates, G. W. Structure-property study of cross-linked hydrocarbon/poly(ethylene oxide) electrolytes with superior conductivity and dendrite resistance. *Chem. Sci.* 2016, 7, 6832–6838.
- [24] Zheng, Q.; Pesko, D. M.; Savoie, B. M.; Timachova, K.; Hasan, A. L.; Smith, M. C.; Miller III, T. F.; Coates, G. W.; Balsara, N. P. Optimizing ion transport in polyether-based electrolytes for lithium batteries. *Macromolecules* 2018, 51, 2847–2858.
- [25] Li, J. C.; Ma, C.; Chi, M. F.; Liang, C. D.; Dudney, N. J. Solid electrolyte: The key for high-voltage lithium batteries. Adv. Energy Mater. 2015, 5, 1401408.
- [26] Croce, F.; Persi, L.; Ronci, F.; Scrosati, B. Nanocomposite polymer electrolytes and their impact on the lithium battery technology. *Solid State Ionics* 2000, 135, 47–52.
- [27] Kim, K. H.; Iriyama, Y.; Yamamoto, K.; Kumazaki, S.; Asaka, T.; Tanabe, K.; Fisher, C. A. J.; Hirayama, T.; Murugan, R.; Ogumi, Z.

- Characterization of the interface between LiCoO₂ and Li₇La₃Zr₂O₁₂ in an all-solid-state rechargeable lithium battery. *J. Power Sources* **2011**, *196*, 764–767.
- [28] Miao, R. R.; Yang, J.; Xu, Z. X.; Wang, J. L.; Nuli, Y.; Sun, L. M. A new ether-based electrolyte for dendrite-free lithium-metal based rechargeable batteries. Sci. Rep. 2016, 6, 21771.
- [29] Ding, F.; Xu, W.; Graff, G. L.; Zhang, J.; Sushko, M. L.; Chen, X. L.; Shao, Y. Y.; Engelhard, M. H.; Nie, Z. M.; Xiao, J. et al. Dendrite-free lithium deposition via self-healing electrostatic shield mechanism. J. Am. Chem. Soc. 2013, 135, 4450–4456.
- [30] Li, W. Y.; Yao, H. B.; Yan, K.; Zheng, G. Y.; Liang, Z.; Chiang, Y. M.; Cui, Y. The synergetic effect of lithium polysulfide and lithium nitrate to prevent lithium dendrite growth. *Nat. Commun.* 2015, 6, 7436.
- [31] Liu, Y. Y.; Lin, D. C.; Li, Y. Z.; Chen, G. X.; Pei, A.; Nix, O.; Li, Y. B.; Cui, Y. Solubility-mediated sustained release enabling nitrate additive in carbonate electrolytes for stable lithium metal anode. *Nat. Commun.* 2018, 9, 3656.
- [32] Mogi, R.; Inaba, M.; Jeong, S. K.; Iriyama, Y.; Abe, T.; Ogumi, Z. Effects of some organic additives on lithium deposition in propylene carbonate. *J. Electrochem. Soc.* 2002, 149, A1578–A1583.
- [33] Yun, Q. B.; He, Y. B.; Lv, W.; Zhao, Y.; Li, B. H.; Kang, F. Y.; Yang, Q. H. Chemical dealloying derived 3D porous current collector for Li metal anodes. *Adv. Mater.* 2016, 28, 6932–6939.
- [34] Lu, L. L.; Ge, J.; Yang, J. N.; Chen, S. M.; Yao, H. B.; Zhou, F.; Yu, S. H. Free-standing copper nanowire network current collector for improving lithium anode performance. *Nano Lett.* 2016, 16, 4431–4437.
- [35] Zhang, Y.; Luo, W.; Wang, C. W.; Li, Y. J.; Chen, C. J.; Song, J. W.; Dai, J. Q.; Hitz, E. M.; Xu, S. M.; Yang, C. P. et al. High-capacity, low-tortuosity, and channel-guided lithium metal anode. *Proc. Natl. Acad. Sci. USA* 2017, 114, 3584–3589.
- [36] Ji, X. L.; Liu, D. Y.; Prendiville, D. G.; Zhang, Y. C.; Liu, X. N.; Stucky, G. D. Spatially heterogeneous carbon-fiber papers as surface dendrite-free current collectors for lithium deposition. *Nano Today* 2012, 7, 10–20.
- [37] Yang, C. P.; Yin, Y. X.; Zhang, S. F.; Li, N. W.; Guo, Y. G. Accommodating lithium into 3D current collectors with a submicron skeleton towards long-life lithium metal anodes. *Nat. Commun.* 2015, 6, 8058.
- [38] Chen, M.; Zheng, J. H.; Sheng, O. W.; Jin, C. B.; Yuan, H. D.; Liu, T. F.; Liu, Y. J.; Wang, Y.; Nai, J. W.; Tao, X. Y. Sulfur–nitrogen co-doped porous carbon nanosheets to control lithium growth for a stable lithium metal anode. *J. Mater. Chem. A* 2019, 7, 18267–18274.
- [39] Tang, L. S.; Zhang, R.; Zhang, X. Y.; Zhao, N. Q.; Shi, C. S.; Liu, E. Z.; Ma, L. Y.; Luo, J. Y.; He, C. N. ZnO nanoconfined 3D porous carbon composite microspheres to stabilize lithium nucleation/growth for high-performance lithium metal anodes. *J. Mater. Chem. A* 2019, 7, 19442–19452.
- [40] Cha, E.; Patel, M. D.; Park, J.; Hwang, J.; Prasad, V.; Cho, K.; Choi, W. 2D MoS₂ as an efficient protective layer for lithium metal anodes in high-performance Li-S batteries. *Nat. Nanotechnol.* 2018, 13, 337–344.
- [41] Yan, K.; Lee, H. W.; Gao, T.; Zheng, G. Y.; Yao, H. B.; Wang, H. T.; Lu, Z. D.; Zhou, Y.; Liang, Z.; Liu, Z. F. et al. Ultrathin two-dimensional atomic crystals as stable interfacial layer for improvement of lithium metal anode. *Nano Lett.* 2014, 14, 6016–6022.
- [42] Xie, J.; Liao, L.; Gong, Y. J.; Li, Y. B.; Shi, F. F.; Pei, A.; Sun, J.; Zhang, R. F.; Kong, B.; Subbaraman, R. et al. Stitching h-BN by atomic layer deposition of LiF as a stable interface for lithium metal anode. Sci. Adv. 2017. 3. eaao3170.
- [43] Liu, Y. Y.; Lin, D. C.; Liang, Z.; Zhao, J.; Yan, K.; Cui, Y. Lithium-coated polymeric matrix as a minimum volume-change and dendrite-free lithium metal anode. *Nat. Commun.* 2016, 7, 10992.
- [44] Luo, J.; Fang, C. C.; Wu, N. L. High polarity poly(vinylidene difluoride) thin coating for dendrite-free and high-performance lithium metal anodes. Adv. Energy Mater. 2018, 8, 1701482.
- [45] Zhang, C.; Lv, W.; Zhou, G. M.; Huang, Z. J.; Zhang, Y. B.; Lyu, R.; Wu, H. L.; Yun, Q. B.; Kang, F. Y.; Yang, Q. H. Vertically aligned lithiophilic CuO nanosheets on a Cu collector to stabilize lithium deposition for lithium metal batteries. Adv. Energy Mater. 2018, 8, 1703404.

- [46] Zhang, N.; Yu, S. H.; Abruña, H. D. Uniform lithium deposition on N-doped carbon-coated current collectors. *Chem. Commun.* 2019, 55, 10124–10127.
- [47] Burns, J. C.; Kassam, A.; Sinha, N. N.; Downie, L. E.; Solnickova, L.; Way, B. M.; Dahn, J. R. Predicting and extending the lifetime of Li-ion batteries. *J. Electrochem. Soc.* 2013, 160, A1451–A1456.
- [48] Adams, B. D.; Zheng, J. M.; Ren, X. D.; Xu, W.; Zhang, J. G. Accurate determination of Coulombic efficiency for lithium metal anodes and lithium metal batteries. *Adv. Energy Mater.* 2018, 8, 1702097.
- [49] Wood, K. N.; Kazyak, E.; Chadwick, A. F.; Chen, K. H.; Zhang, J. G.; Thornton, K.; Dasgupta, N. P. Dendrites and pits: Untangling the complex behavior of lithium metal anodes through *operando* video microscopy. ACS Cent. Sci. 2016, 2, 790–801.
- [50] Wang, X.; Zeng, W.; Hong, L.; Xu, W. W.; Yang, H. K.; Wang, F.; Duan, H. G.; Tang, M.; Jiang, H. Q. Stress-driven lithium dendrite growth mechanism and dendrite mitigation by electroplating on soft substrates. *Nat. Energy* 2018, 3, 227–235.
- [51] Liu, W.; Li, W. Y.; Zhuo, D.; Zheng, G. Y.; Lu, Z. D.; Liu, K.; Cui, Y. Core-shell nanoparticle coating as an interfacial layer for dendrite-free lithium metal anodes. ACS Cent. Sci. 2017, 3, 135–140.

- [52] Zhang, X. Q.; Cheng, X. B.; Chen, X.; Yan, C.; Zhang, Q. Fluoroethylene carbonate additives to render uniform Li deposits in lithium metal batteries. Adv. Funct. Mater. 2017, 27, 1605989.
- [53] Mueller, F.; Geiger, D.; Kaiser, U.; Passerini, S.; Bresser, D. Elucidating the impact of cobalt doping on the lithium storage mechanism in conversion/alloying-type zinc oxide anodes. *ChemElectroChem* **2016**, *3*, 1311–1319.
- [54] Varzi, A.; Mattarozzi, L.; Cattarin, S.; Guerriero, P.; Passerini, S. 3D porous Cu-Zn alloys as alternative anode materials for Li-Ion batteries with superior low t performance. Adv. Energy Mater. 2018, 8, 1701706.
- [55] Jin, C. B.; Sheng, O. W.; Luo, J. M.; Yuan, H. D.; Fang, C.; Zhang, W. K.; Huang, H.; Gan, Y. P.; Xia, Y.; Liang, C. et al. 3D lithium metal embedded within lithiophilic porous matrix for stable lithium metal batteries. *Nano Energy* 2017, 37, 177–186.
- [56] Zhang, R.; Chen, X. R.; Chen, X.; Cheng, X. B.; Zhang, X. Q.; Yan, C.; Zhang, Q. Lithiophilic sites in doped graphene guide uniform lithium nucleation for dendrite-free lithium metal anodes. *Angew. Chem.*, Int. Ed. 2017, 56, 7764–7768.
- [57] Okamoto, H. Li-Zn (lithium-Zinc). J. Phase Equilib. Diff. 2012, 33, 345–345.